Applied Clay Science 259 (2024) 107515

Contents lists available at ScienceDirect

Applied Clay Science

journal homepage: www.elsevier.com/locate/clay

Research Paper

# Thermal activation of kaolinite through potassium acetate intercalation: A structural and reactivity study

Adrian Alvarez-Coscojuela, Josep Marco-Gibert, Jofre Mañosa, Joan Formosa, Josep Maria Chimenos *

*Departament de Ciència de Materials i Química Física, Universitat de Barcelona, Martí i Franquès 1, 08028 Barcelona, Spain*

ARTICLE INFO

*Keywords:*
Kaolin intercalation
Pozzolanic activity supplementary cementitious materials
Alternative cementitious materials
Dehydroxylation

ABSTRACT

Calcined clays have emerged as a suitable alternative to partially replace conventional cement due to their high pozzolanic activity. This study explores a novel activation methodology for kaolinite, aiming to obtain metakaolin at lower temperatures than conventional thermal activation. This methodology involves a prior intercalation stage with potassium acetate (KAc) before thermal activation. The effectiveness of KAc intercalation was assessed through X-ray diffraction (XRD), indicating an intercalation ratio of approximately 90%. Several calcined temperatures were tested in accordance with the thermal behaviour analyzed through thermogravimetric analysis (TGA). Once calcined, the intercalated kaolinites exhibited enhanced reactivity compared to conventional calcined clays in the range between 400 °C to 550 °C, as demonstrated by modified Chapelle and Si/Al availability tests. A comprehensive structural characterization was conducted to facilitate a better understanding of the novel KAc-based metakaolin reactivity through various techniques (XRD, $^{27}$Al - $^{1}$H MAS NMR, and TGA). This focused on the crystalline changes in the kaolinite structure, the evolution of Al atoms conformation, and the OH behaviour at different thermal activation temperatures. Overall, this study highlights the potential of KAc intercalation as a strategy to obtain higher metakaolin content at lower temperatures than through conventional thermal treatments, offering insights into the development of its potential use as supplementary cementitious materials or alternative cementitious materials precursor.

## 1. Introduction

Ordinary Portland cement (OPC) production entails a significant contribution to carbon dioxide emissions worldwide (Gartner, 2004; Scrivener et al., 2018) The production of one cement tonne leads to 900 kg $CO_2$ emission (Benhelal et al., 2013). To keep the global environmental balance, the cement research community has been pressured to develop new eco-friendly construction materials (Schneider et al., 2018). For this purpose, calcined clays rise as a suitable option as an interesting replacement for conventional cement (Sabir et al., 2001). Calcining kaolin (K) in the range between 700 and 800 °C produces the dehydroxylation of kaolinite (Kaol) structure, which highly disorders its crystalline composition. The obtained aluminosilicate 3-dimensional framework, named metakaolin (MK), possesses a high pozzolanic activity in contact with $Ca(OH)_2$, forming various cementitious phases (Siddique and Klaus, 2009; Ramezanianpour and Bahrami Jovein, 2012). The high reactivity of MK promotes its implementation in several cementitious materials either as alternative cementitious materials (ACM) or as supplementary cementitious materials (SCM) (Fernandez et al., 2011; Tironi et al., 2012, 2013).

Kaolinite $Al_2[Si_2O_5](OH)_4$ (see Fig. 1), the MK precursor, exhibits remarkable versatility in reactivity terms. Kaol can interact with both organic and inorganic substances through adsorption, intercalation, and cation exchange mechanisms (Brigatti et al., 2013). Notably, the intercalation of organic molecules into Kaol layers emerges as a compelling area of interest within the field of clay research. The intercalation phenomenon involves the insertion of guest organic molecules into the interlamellar spacing of Kaol, thereby disrupting the hydrogen bond network between the Si—Al oxide layers (Deng et al., 2002). This process results in an expansion of Kaol interlayer distance (Li et al., 2009; He et al., 2014).

A wide number of organic molecules with intercalation properties, such as hydrazine, potassium acetate, dimethyl sulphoxide, urea, or formamide, have been studied in recent years (Horváth et al., 2010;

---

* Corresponding author.
*E-mail address:* chimenos@ub.edu (J.M. Chimenos).

https://doi.org/10.1016/j.clay.2024.107515
Received 30 April 2024; Received in revised form 23 June 2024; Accepted 26 July 2024

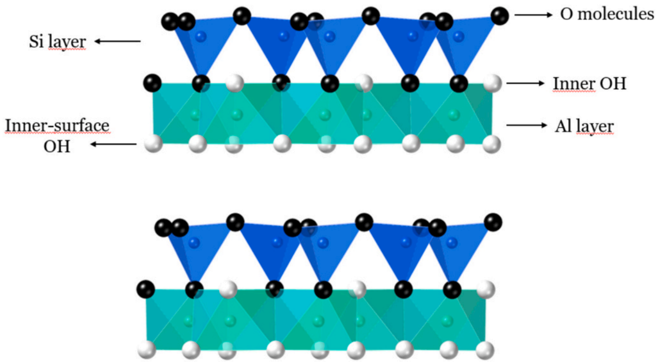

**Fig. 1.** Schematic Kaol structure.

Lagaly et al., 2013). According to the literature, intercalation procedures require long reaction times (Lagaly et al., 2013). In this regard, among all organic guest options, the intercalation of potassium acetate (KAc) has been reported to require the shortest reaction times (~1 day) (Cheng et al., 2010a). Furthermore, KAc insertion on Kaol layers has also demonstrated the highest reaction degrees (Ruiz Cruz, 1999).

Intercalating processes change Kaol thermal behaviour (Horte et al., 1988; Gabor et al., 1995; Cheng et al., 2012b). There are different studies supporting that the thermal decomposition of KAc-intercalated Kaol (K-KAc) takes place at lower temperatures than unaltered Kaol (Cheng et al., 2012a; Zhong et al., 2017). The onset of Kaol dehydroxylation occurs at ~450 °C, whereas for the K-KAc intercalated systems, the dehydroxylation starts at around 300 °C (Cheng et al., 2014; Mako et al., 2014). Despite the very limited application of KAc intercalation in the cement industry (Zeng et al., 2014), the thermal performance of K-KAc complexes may lead to an improved thermal activation methodology for the production of SCM or cement precursors for ACM.

In this sense, this work aims to achieve MK at lower temperatures than through the conventional thermal activation procedures. This innovative activation methodology involves a preliminary chemical treatment with KAc prior to thermal activations. This multi-step process may enhance the pozzolanic activity at lower temperatures compared to conventional calcined clays. Firstly, the reaction degree of the KAc insertion was assessed and quantified. After different calcination treatments, reactivity measurements were carried out to evaluate the effectiveness of this novel activation method. Then, a comprehensive structural characterization was conducted to elucidate the reactivity variations. Non-intercalated kaolinites were also studied for comparison purposes.

## 2. Materials and methods

### 2.1. Materials

The raw kaolinitic clay employed for intercalating was supplied by the Spanish company Minerals i Derivats, S.A and was used without any further purification. Its chemical composition was determined by X-ray fluorescence (Table 1) with a Panalytical Philips PW 2400 sequential X-ray spectrophotometer equipped with UniQuant® V5.0 software. The crystalline composition was evaluated by means of X-ray diffraction (XRD) using a Bragg-Brentano PANalytical X'Pert PRO MPD alpha1 powder diffractometer with CuKα1 radiation (λ = 1.5406 Å). The measuring time was 100 s and five scans were performed for each sample. The experimental setup included a focusing Ge (111) primary monochromator, with a step size of 0.026°, an anti-scatter slit of 4° and a Soller slit of 0.04 rad. The main crystalline phases of raw kaolin were analyzed using the X'Pert HighScore software. Potassium acetate (KAc) used for the intercalation process was provided by Panreac.

To carry out the pozzolanic tests, the purchased reagents were calcium oxide and sodium hydroxide from Thermoscientific, and D(+)–Sucrose AGR and hydrochloric acid 0,1 N from Labkem for the titrations.

### 2.2. Methods and characterization techniques

#### 2.2.1. Intercalation methodology

The intercalated complexes were prepared by directly combining raw kaolin with a 7.2 M KAc solution for 24 h. The reaction system comprised a reflux column and was exhaustively stirred at 60 °C with a solid-to-liquid ratio of 1:5. Once the reaction ended, the resulting paste was filtered, and the resultant solid was dried at 105 °C for 2 days of ageing. Subsequently, the solid was washed with ethanol to remove any excess of non-intercalated KAc. Nonetheless, the authors preferred to assume a small loss in the intercalation ratio over a remaining significant amount of KAc, which would generate too much $CO_2$ when calcined.

For the intercalation effectiveness measurements, X-ray diffraction (XRD) was employed. PANalytical X'Pert PRO MPD alpha1 powder diffractometer in Bragg-Brentano θ/2θ geometry of 240 mm of radius (CuKα1 radiation, λ = 1.5406 Å). The work power used was 45 kV – 40 mA. A focusing Ge (111) primary monochromator was used for the measurements. The preparation via of the samples was back-loading. The intercalation extent was determined by the intercalation ratio (IR), which was calculated using the intensity values of the 001 reflection (basal reflection) as stated in Eq. (1). For this purpose, the X'Pert HighScore software was used to determine the relative intensity data.

$$IR = \frac{I(001)\ intercalated\ kaolinite}{[I(001)\ intercalated\ kaolinite + I(001)\ kaolinite]} \cdot 100 \tag{1}$$

Scanning electron microscopy (SEM) was employed to compare the intercalated clay with raw kaolin. For this purpose, the samples were coated with carbon and scanned using a JEOL J-7001F microscope, operating at a 15 kV accelerating voltage. In addition, a thermogravimetric analysis (TGA) was conducted to analyze the intercalation using an SDT Q600 (TA Instruments) from 30 to 800 °C, with a heating rate of 10 $°C{\cdot}min^{-1}$ and a synthetic air flux of 50 $mL{\cdot}min^{-1}$.

#### 2.2.2. Calcination series

Once the intercalation was achieved, intercalated kaolinites were calcined at 400, 450, 500, 550, and 600 °C for 2 h to evaluate any potential increase in the reactivity of the thermal activated Kaol. They were calcined heating in-situ from room temperature 5 g each sample using a Hobersal JB20 muffle furnance (maximum temperature of 1100 °C).The calcination series were also carried out for the raw kaolin for comparison purposes. The nomenclature of the samples through this work was K-T or KI-T, where K or KI were assigned to raw kaolin or intercalated kaolinite, respectively, whereas T denotes the temperature applied during the thermal process.

#### 2.2.3. Clay activity assessment

*Modified Chapelle test:* 1 g of calcined clays (both K-T and KI-T series) and 2 g of powdered CaO were added to 250 mL of distilled water (Li et al., 2018). The mixture was then vigorously stirred for 16 h at 90 °C controlled by refrigerant equipment (Ferraz et al., 2015). A control

**Table 1**
XRF analysis of the raw kaolin.

| Compounds | $SiO_2$ | $Al_2O_3$ | $K_2O$ | $Fe_2O_3$ | CaO | $TiO_2$ | $Na_2O$ | MgO | $P_2O_5$ | LOI* |
|---|---|---|---|---|---|---|---|---|---|---|
| wt% | 49.85 | 36.31 | 0.69 | 0.47 | 0.16 | 0.15 | 0.13 | 0.11 | 0.08 | 12.03 |

[*] LOI: Loss on ignition at 1100 °C.

experiment (blank test) without the pozzolanic material was made under the same conditions. Once the reaction system cooled down for 1 h, the solution was added to 250 mL of sucrose 0.7 M and mixed for 15 min. Then, approximately 150 mL of the reacting system-sucrose resultant solution was filtrated, and 25 mL were titrated with 0.1 M HCl and 3 phenolphthalein drops. To measure the portlandite ($Ca(OH)_2$) fixed by the SCM, the following formula was used:

$$PA = 2\cdot\frac{v1 - v2}{v1}\cdot\frac{74}{56}\cdot 1000 \tag{2}$$

where PA (pozzolanic activity) denotes the mg of fixed $Ca(OH)_2$·per g of SCM ($mg\cdot g^{-1}$), $v1$ is the required volume for titrating 25 mL of control solution, and $v2$ is the required volume for titrating 25 mL of the solution where the pozzolanic reaction takes place.

*Availability of Si and Al test:* The $SiO_2$ and $Al_2O_3$ availability was investigated employing Inductively Coupled Plasma – Optical Emission Spectroscopy (ICP-OES) on the resultant solution derived from chemical treatments using 8 M NaOH (Mañosa et al., 2022). 1 g for each K-Ts and KI-Ts was solved in 100 mL of 8 M NaOH (solid-to-liquid ratio of 1/100). This system was stirred for 5 h at 80 °C. Three replicates were made to ensure repeatability.

### 2.2.4. *Structural characterization of the resultant calcined clays (K-Ts and KI-Ts)*

The Fourier-transform infrared spectroscopy (FTIR) was employed to evaluate the acetate removal and the structural evolution of the calcined intercalated Kaol, with 32 scans over the range of 4000–450 $cm^{-1}$ at a resolution of 4 $cm^{-1}$. For this purpose, the A Spectrum Two™ PerkinElmer spectrometer in attenuated total reflectance (ATR) mode was used. The spectra were enclosed to the interest scanning regions. Furthermore, TGA was carried out to track the removal of OH groups in order to study the intercalation effect on the dehydroxylation rate of the K and KI series. X-ray diffraction was also employed to evaluate the crystalline evolution of kaolinite reflections, using the same conditions described above (section 2.2.1.). Solid state $^{27}Al$ MAS-NMR (magic angle spinning nuclear magnetic resonance) was implemented to follow the structural disorder exhaustively through the Al coordination numbers evolution. Its spectra were recorded at RT in an AVANCEIII HD 600 (Bruker AXS) spectrometer using a double resonance CPMAS probe of 4.0 mm at a spinning rate of 13 kHz. The magnetic field was 14.1 T corresponding to a $^{27}Al$ resonance frequency of 156.37 MHz. The $^{27}Al$ chemical shifts are referenced to $Al(NO_3)_3$. $^{27}Al$ MAS-NMR spectra were recorded with an excitation pulse of 0.7 μs and 1-s delay with $^{1}H$ decoupling ($^{27}Al$ Hpdec with spinal 64 decoupling sequence for Al) and summing up 2000 scans. $^{1}H$ MAS-NMR spectra were recorded at RT in an AVANCEIII HD 600 (Bruker AXS) spectrometer using a triple resonance DVT probe of 2.5 mm at a spinning rate of 25 kHz to compare the OH evolution between calcined intercalated and non-intercalated kaolinites at each temperature. The magnetic field was 14.1 T corresponding to a $^{1}H$ resonance frequency of 600.09 MHz. The $^{1}H$ chemical shifts are referenced to adamantane. $^{1}H$ MAS NMR spectra were recorded with an excitation pulse of 2 μs and 3-s delay summing up 64 scans.

## 3. Results and discussion

### 3.1. *K-KAc intercalation assessment*

Fig. 2 depicts the diffractogram patterns of both the raw kaolin and the intercalated kaolinite, providing insight into its structural evolution. The utilization of the XRD technique is commonly employed to evaluate the effectiveness of intercalation, as noted in previous studies (Li et al., 2009; Cheng et al., 2010b). The intercalation procedure leads to an expansion of the interlayer space of Kaol along the normal direction to the (001) crystal plane (Cheng et al., 2015). The interlayered extension varies depending on the organic guest proposed. In this KAc studied case, the intercalation induces an interlamellar expansion from 0.706 Å to 1.416 Å, altering the typical 001 reflection (basal reflection) from 12.5° to 6.2°. The appearance of this new peak indicates that the potassium acetate molecules are straightly inserted into the lamellar space of Kaol. The intercalation degree for the K-KAc complex of this experimental procedure was assessed through the reflection intensities, following Eq. (1). The insertion was achieved with an efficiency of 89%. As previously mentioned, K-KAc complexes appear to be the most efficient intercalation in yield terms as they result in the largest basal spacings. Nonetheless, the utmost level of reaction may not consistently reach 100%, even after prolonged reaction durations, as this is contingent upon the nature of K, structural order, and particle size (Gabor et al., 1995; Ruiz Cruz, 1999). Moreover, inner OH may not contribute to intercalation as inner-surface OHs (see Fig. 1) since they are not located in the interlayer space.

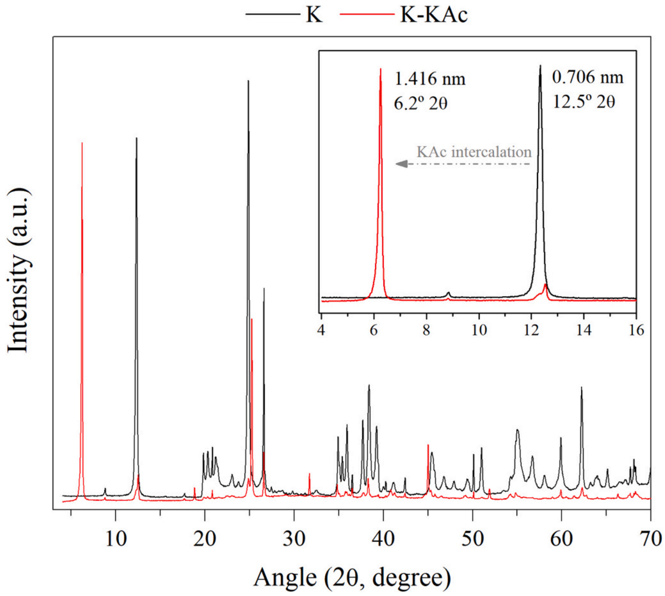

**Fig. 2.** XRD patterns of raw kaolin (K) and K-KAc complex with a focused diffractogram on 4° to 16° region.

The kaolinite and KAc-intercalated kaolinite SEM images are presented with different magnifications in Fig. 3. The crystalline kaolinite in the raw kaolin is formed by pseudo-hexagonal plates disposed of laminarly, building an accordion structure with sharp edges (San Cristóbal et al., 2010; Cheng et al., 2018; Mañosa et al., 2023). These stacked films are presented in both Fig. 3a-b, revealing a high crystalline degree for the Kaol studied. On the other hand, a morphological change is observed once the intercalation has been accomplished. Fig. 3c shows that the kaolinitic films are appreciably distorted and more randomly distributed, changing the initial conformation of kaolinite. This may be because the intercalation reaction breaks the interlayered hydrogen bonds, thereby disrupting the kaolinitic structure. In addition, even the kaolinitic crystalline network is disrupted due to the KAc insertion, as seen in Fig. 2, the layers set remained with the lamellar disposition (see Fig. 3c).

A thermogravimetric analysis is implemented to foresee the thermal behaviour of KAc intercalated. It is well-known that the kaolinite dehydroxylation process produces around 13 wt% loss between the range of 400–700 °C, which provides higher reactivity to the material by amorphizing it (Shvarzman et al., 2003; Johnston et al., 2022). For the K sample studied (see Fig. 4, black line), 12.1% of mass loss is reached. The dehydroxylation depends on the particle size, quantity of impurities, and heating rate, among others (Alfonso et al., 2022) as well as the percentage of Kaol in the K. The differential thermogravimetry curve (DTG) curve marked the peak at 520 °C.

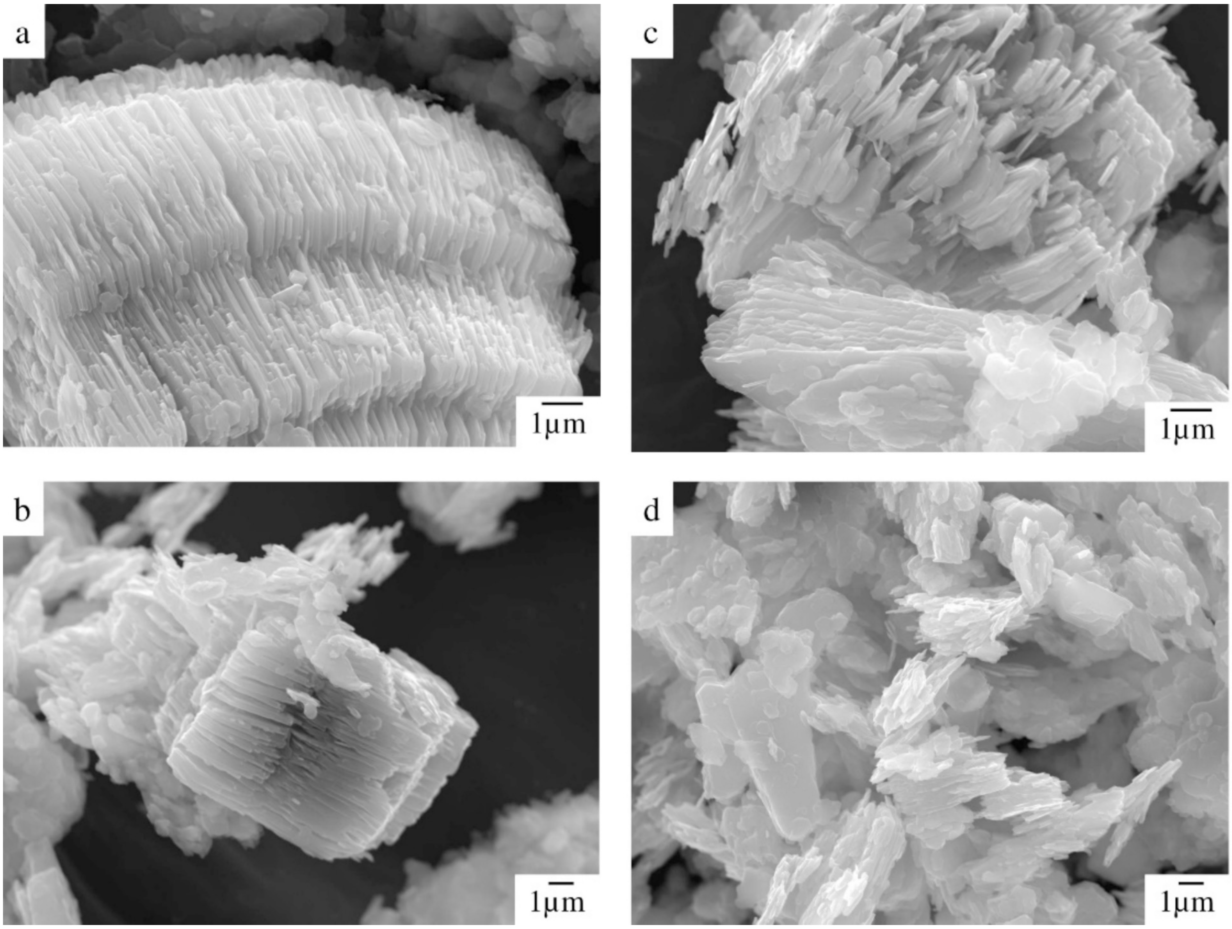

**Fig. 3.** SEM micrographs of raw K (a-b) and KAc-intercalated complex (c-d).

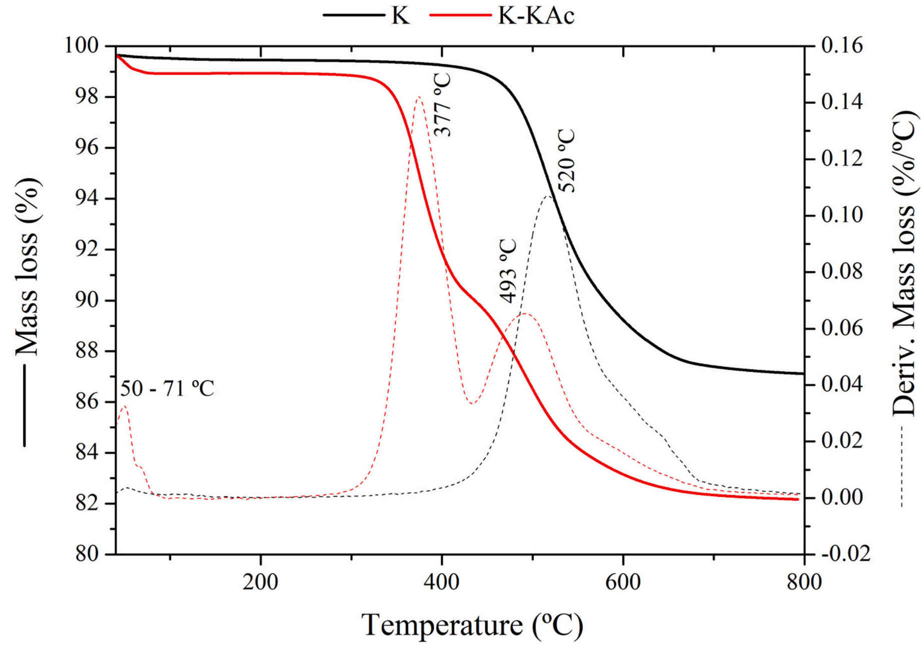

**Fig. 4.** Thermogravimetric analysis (TGA) and differential thermogravimetric (DTG) curves of K and K-KAc composite.

Contrarily, there are many discrepancies in the literature regarding the dehydroxylation in intercalated kaolinite composites (Mako et al., 2014; Zeng et al., 2014; Cheng et al., 2015; Zhong et al., 2017). The thermal behaviour varies depending on the degree of intercalation. In any case, backtracking on the temperature of dehydroxylation is experimented for the K-KAc complex (see Fig. 4, red line) in comparison with K, according to DTG curves. TGA shows two distinct steps of mass loss at 377 °C and 493 °C, assigned to acetate decomposition and OHs dehydroxylation, respectively. This may be due to the kaolinitic interlayer distance expansion caused by intercalation. This process exposes the OH groups, predisposing them to a more thermally efficient activation. In addition, the crystallinity of kaolinite decreases sharply after intercalation. As a result of both phenomena, a more rapid onset of dehydroxylation results from intercalated kaolinites. The first small weight loss is attributed to the moisture content of the tested sample.

### 3.2. *Reactivity measurements*

The modified Chapelle test (Fig. 5) evaluates the pozzolanity acquirement of the K and KI series through thermal activations. The capability of the calcined clays to react with $Ca(OH)_2$ by consuming calcium defines its potential reactivity. An interesting pattern is appreciated in the lower calcination temperatures used. An increase in the reactivity for KI-400, 450, and 500 in comparison with K-400, 450, and 500 was obtained. Thus, K-400 consumed 0.23 g, while KI-400 consumed 0.43 g. K-450 consumed 0.25, while KI-450 consumed 0.62 g. K-500 consumed 0.84 g, while KI-500 consumed 1.15 g. The most notable difference was observed in the KI-450 sample, which exhibited an increase in reactivity to almost 250% concerning K-450. The intercalation of kaolinite as a previous procedure to produce metakaolin allows to achieve a more reactive material than conventional kaolinite calcined at the same temperature between 400 and 500 °C. Nonetheless, at temperatures of 550 °C and 600 °C, both the K and KI series reached similar ranges of calcium consumption values. This indicates that once the dehydroxylation is fully accomplished for both kaolinitic series, their reactivity performances become equal, with the consumption of portlandite falling within the 1.4 to 1.7 g range.

To furnish evidence of the reactivity behaviour, chemical extractions of Si and Al in a concentrated NaOH solution were carried out (Fig. 6). Even though this test is typically used to evaluate the potential aluminosilicate source application as an alkali geopolymer, the Si and Al availability can also determine the potential pozzolanity as well (Kuenzel and Ranjbar, 2019). The dissolved content is expressed as available $SiO_2$ and $Al_2O_3$ relative to the total $SiO_2$ and $Al_2O_3$ content in the raw kaolin, respectively. The trend of Al and Si dissolution behaviour remained almost consistent across different calcination temperatures, with only very slight variations. This suggests that the same quantity of aluminates and silicates are potentially reactive units. Intensifying the thermal activation promotes more reactive $SiO_2$ and $Al_2O_3$ particles as the degree of dehydroxylation and amorphisation increases (Bich et al., 2009). Consequently, an increase in the dissolution of Si and Al particles in the alkali medium was observed as the thermal treatment temperature increased. Hence, the results also agreed with the Modified Chapelle test.

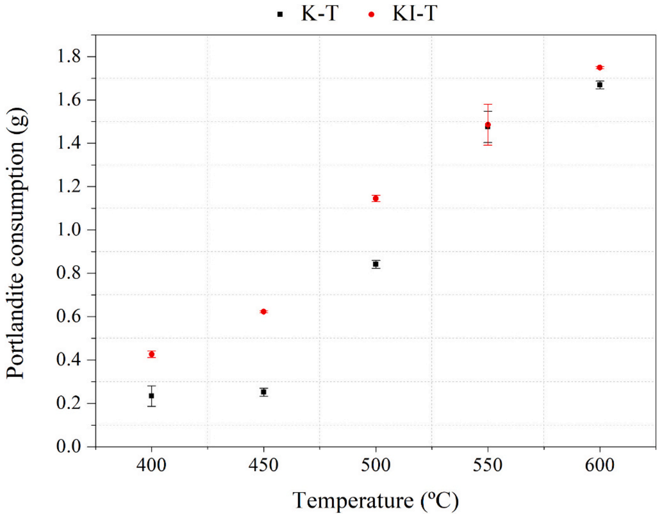

**Fig. 5.** Consumed portlandite in the modified Chapelle test for K-T and KI-T series.

Based on the ICP analysis of the supernatant, the Si and Al dissolution are higher in the calcined intercalated kaolinites compared to the calcined non-intercalated kaolinites. This indicates a higher degree of amorphization in the intercalated samples, suggesting enhanced reactivity due to the structural changes induced by intercalation. A trend is observed for aluminates and silicates at 400, 450 and 500 °C. When the intercalated-kaolinites are submitted under calcination, the dehydroxylation takes place more readily due to a higher exposal of the OHs and the structure disruption (caused by KAc intercalation) than the raw kaolin (Cheng et al., 2012a). Hence, more available Si and Al units are obtained for intercalated complexes calcined at the same temperature than non-intercalated kaolinites. On the other hand, at 550 °C, even though the intercalated complex still shows a higher reactive content of $SiO_2$ and $Al_2O_3$ than the non-intercalated, the reactivity values are much closer than in lower calcinating temperatures. Moreover, at 600 °C the dissolved content values are slightly increased for the K-600 in comparison to KI-600. Nonetheless, the values still fall within a similar, relatively narrow range, suggesting a convergence in reactivity at this higher temperature. This potential plateau reached is explained as follows: the reactivity values are defined by the dehydroxylation degree. Once OH removal is entirely accomplished, the amorphization levels of the aluminosilicates can not increase notably, and neither can its reactivity. This is in accordance with the modified Chapelle test results. The presence of potassium from KAc could slightly alter the reactivity of metakaolin (Xu et al., 2011).

### 3.3. *Structural characterization of the resultant calcined clays (K-Ts and KI-Ts)*

The intercalated Kaol (denoted as K-KAc in Fig. 7a) exhibits characteristic acetate bands in the FTIR spectrum. Specifically, the band at 1336 $cm^{-1}$ corresponds to $CH_3$ deformation, whereas those at 1401 $cm^{-1}$ and 1569 $cm^{-1}$ are attributed to symmetric and antisymmetric C═O stretching, respectively (Xu et al., 2015). The FTIR analysis thus confirms the intercalation process. When the intercalated complex is treated at 400 °C (KI-400), all acetate anions are removed from the structure, as evidenced by the complete disappearance of these bands. This removal is consistent for samples K-450, K-500, K-550, and K-600, indicating that thermal treatments effectively eliminate the intercalated acetate. In the region from 750 $cm^{-1}$ to 1100 $cm^{-1}$, bands corresponding to Si—O, Al—O, and Si-O-Al vibrations in Kaol show broadening with progressive thermal treatment of the K-KAc complex. This broadening is indicative of kaolinitic structural amorphization, as previously reported (Alvarez-Coscojuela et al., 2024). Fig. 7b highlights the FTIR spectral region of hydroxyl groups, where new bands appear at 3450 $cm^{-1}$ and 3600 $cm^{-1}$. These correspond to the hydroxyl stretching of interlayer water coordinated to acetate and the stretching of inner hydroxyl groups in Kaol aligned parallel to the (001) direction, respectively (Frost et al., 2001). Additionally, bands at 3688 $cm^{-1}$, 3670 $cm^{-1}$, 3653 $cm^{-1}$, and 3620 $cm^{-1}$ are associated with hydroxyl group vibrations (Mañosa et al., 2023). Thus, since none of the KI-T samples exhibit acetate vibrations, it can be concluded that acetate is completely eliminated at all studied calcination temperatures. Furthermore, the FTIR data indicates that hydroxyl groups are almost fully removed at 500 °C when intercaled.

Fig. 8 was implemented to track the OH content (%) of the K-T and KI-T series to compare the dehydroxylation degree between them. For clearer visual representation, TGA data was adjusted to show 100% mass loss at 400 °C. This normalization allows for a more straightforward comparison of the rate and extent of dehydroxylation in each series, highlighting differences in thermal behaviour and chemical reactivity due to the presence or absence of intercalation. The mass loss attributed

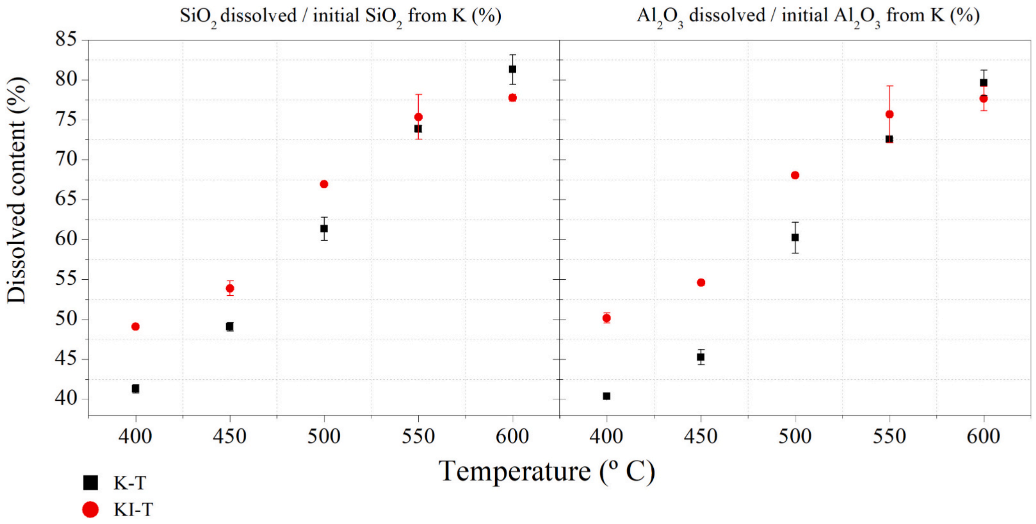

**Fig. 6.** The percentage of $SiO_2$ and $Al_2O_3$ availability relative to the total $SiO_2$ and $Al_2O_3$ content in the raw kaolin, as identified by XRF (Table 1).

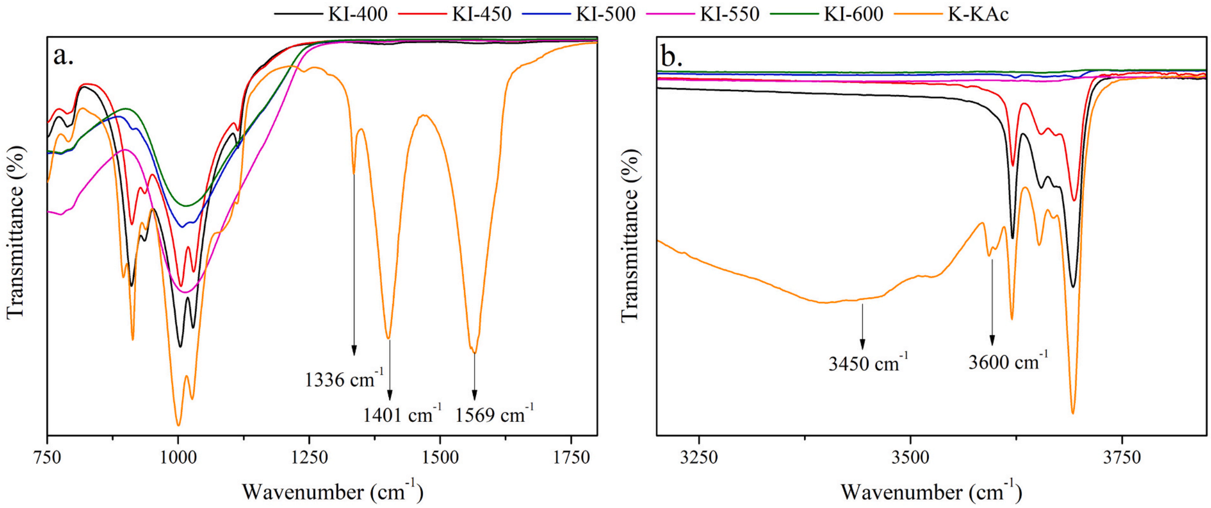

**Fig. 7.** FTIR of K-KAc complex and the KI-T serie.

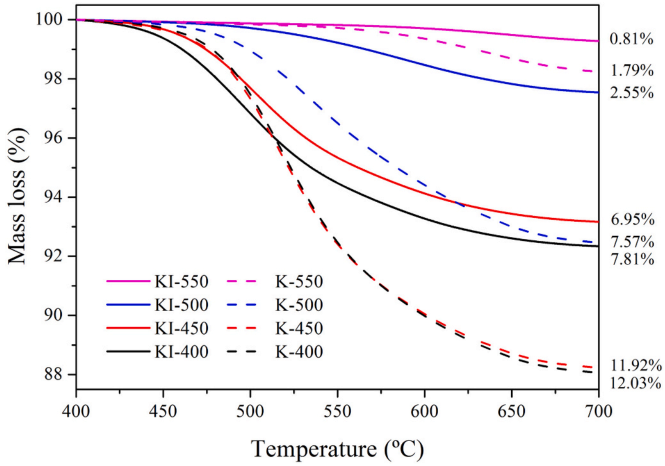

**Fig. 8.** Thermal behaviour of K-T and KI-T series calcined at 400, 450, 500, and 550 °C.

to all samples between 400 °C to 700 °C is located on the right side of the figure, which corresponds to kaolinite dehydroxylation since the acetate is already eliminated at 400 °C, as evidenced through FTIR. Table 2 displays the degree of dehydroxylation as the percentage of hydroxyls removed during calcination. This percentage is calculated based on the difference between the mass loss from the dehydroxylation of thermally treated samples and the mass loss from the dehydroxylation of raw kaolin (12.1%, as seen in Fig. 4).

The Kaol dehydroxylation in the K series does not occur significantly

**Table 2**
Degree of dehydroxylation of K and KI series.

| | Mass loss from TGA (wt%) | Degree of dehydroxylation (%) |
|---|---|---|
| K | 12.10 | – |
| K-400 | 12.03 | 0.58 |
| K-450 | 11.92 | 1.49 |
| K-500 | 7.57 | 37.44 |
| K-550 | 1.79 | 85.21 |
| KI-400 | 7.81 | 35.45 |
| KI-450 | 6.95 | 42.56 |
| KI-500 | 2.55 | 78.93 |
| KI-550 | 0.81 | 93.31 |

until the temperature reaches at least 450 °C. According to TGA data, the K-400 and K-450 mass loss is almost negligible, which is consistent with Fig. 4. At 500 °C, a 7.57% mass loss is achieved on the TGA, which means losing 37.44% of all available OHs. Simultaneously, at 550 °C the mass loss value of TGA results in 1.79%. The OH loss from calcination of K-550 reaches 85.21% of the total OHs. On the other hand, the intercalated-kaolinite displays a higher degree of dehydroxylation at the same temperature calcination than the K dehydroxylation. Comparing the OHs removed percentage of K-T and KI-T series, calcining raw kaolin at 500 °C and intercalated kaolinite at 400 °C results in a ~ 36–38% of dehydroxylated OHs, which means avoiding 100 °C to achieve the same dehydroxylation values. Furthermore, comparing K-400 and K-450 with KI-400 and KI-450, a significant difference can be observed between the total OH removal. In addition, KI-500 doubles the dehydroxylation rate compared to K-500.

Fig. 9 depicts the crystalline evolution of both intercalated and non-intercalated Kaol samples in the low-angles region, as it comprises the most intense kaolinitic reflections. XRD was performed as a key technique to track the amorphization degree to further understand the reactivity results. Both series of samples presented some variations in comparison with the raw kaolin (Fig. 2) since the thermal treatment of kaolinitic structures promotes its distortion, leading to a diminishment of the kaolinitic reflections. It is also remarkable that KAc intercalated particles are removed from every sample since the 6.2° reflection returned to 12.5° in all XRD spectra. This means that, at 400 °C, the potassium acetate intercalated is effectively eliminated, suggesting complete decomposition of the intercalant at this temperature. Comparing K-400 and KI-400, a substantial intensity reduction on 12.5° and 24.9° angles is observed. This pattern is also repeated with calcination at 450, 500 and 550 °C. Furthermore, as the diminishment of the kaolinitic reflections at 12.5° and 24.9° are more readily observed than the reflections enclosed on the 17–23° region, the authors have provided higher-resolution spectra (Fig. A1) to facilitate a clearer analysis of these changes. Nonetheless, the spectra do not vary so much at 550 °C, because for the non-intercalated complexes, the dehydroxylation is almost achieved too. Therefore, the intercalation process is more useful at low temperatures in order to obtain the new SCM-ACM. In addition, quartz and illite remain stable since the intercalation process only affects kaolinitic structures, and the treatment at the temperature does not involve any processes that could significantly alter their crystalline structure. Hence, no variation is observed in these reflections.

In structural terms, the X-ray diffraction analysis revealed a significant decrease in the crystalline structure of the intercalated kaolinite complexes compared to non-intercalated kaolinite at the same thermal activation temperature. This is consistent with the higher reactivity accomplished by intercalated compounds in front of the non-intercalated, represented in Fig. 5 and Fig. 6.

The aluminium sheet is directly bonded to the hydroxyl groups; when those are eliminated through dehydroxylation, the Al suffers modifications on its conformation, which can be monitored by aluminium magic-angle spinning nuclear magnetic resonance spectroscopy ($^{27}$Al MAS NMR). Metakaolin (see MK in Fig. 10a) was added for comparison purposes. It is obtained through calcination at 800 °C. The aluminium environments of Kaol and MK, illustrated in Fig. 10b, are discerned through $^{27}$Al MAS NMR. In the K spectrum, the pronounced appearance of a sharp peak at 4.7 ppm affirms the presence of hexacoordinated Al, which is indicative of the typical Al surroundings for the crystalline Kaol structures (Walkley and Provis, 2019). Minor contributions from K-feldspars (around 60 ppm) and illite (around 70 ppm) are also observed (Mañosa et al., 2022). The MK spectrum reveals three distinct resonances at 4.7 ppm, 30.7 ppm, and 56.6 ppm, corresponding to Al$^{VI}$, Al$^{V}$, and Al$^{IV}$, respectively (Alvarez-Coscojuela et al., 2024). The acquisition of Al$^{IV}$ and Al$^{V}$ units implies a significantly amorphized Kaol structure.

Concerning the K-T and KI-T series, Fig. 10c-d plots the Al evolution through calcination at 450 °C and 500 °C. When comparing KI-T and K-T calcined at the same temperature some variations in the Al surroundings are observed, which are directly related to its potential reactivity. At 450 °C (Fig. 10c), K-450 does not experiment with any remarkable change, whereas KI-450 undergoes an Al$^{VI}$ to Al$^{IV}$ slight conversion, indicating a higher amorphization level and the start of the dehydroxylation process. At 500 °C (Fig. 10d), there is a significant increase in the presence of Al$^{IV}$ and Al$^{V}$, as well as Al$^{VI}$ decreased for KI sample. This indicates a substantial transformation in Al coordination within the intercalated kaolinite structure towards lower coordination states, suggesting enhanced amorphization. Conversely, for the Kaol samples at the same temperature, while there is evidence of dehydroxylation indicated by the small presence of Al$^{IV}$ and Al$^{V}$, the main Al conformation remains as Al$^{VI}$, as kaolinitic crystalline structure. The quantity of Al$^{IV}$ and Al$^{V}$ is severely increased in KI-500 in comparison to K-500, hence its amorphization degree and reactivity. According to XRD and $^{27}$Al MAS NMR studies, for the same calcination temperature, KI-T series suffers more structural changes than K-T series. Consequently, the intercalation method enhances the generation of amorphous content using the same

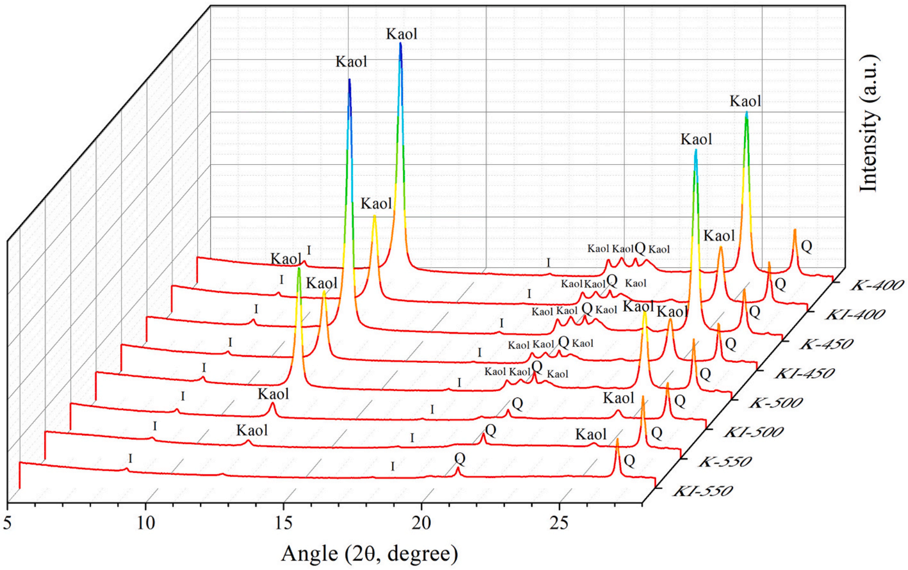

**Fig. 9.** Comparative XRD for calcined kaolinite and calcined intercalated kaolinite at 400 °C, 450 °C, 500 °C, 550 °C. Kaol = Kaolinite, Q = Quartz, and I=Illite.

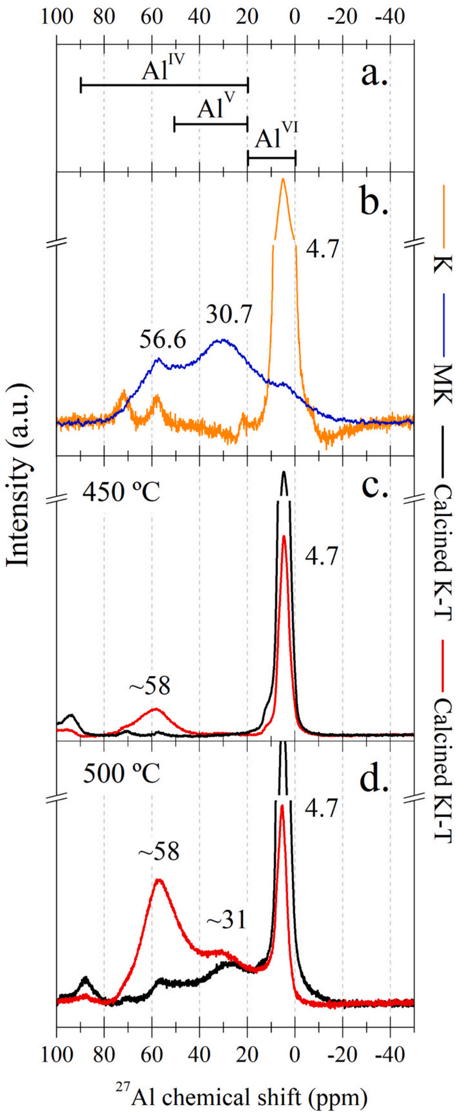

**Fig. 10.** Solid-state NMR of $^{27}$Al (a) of Kaol and MK (b), K-450 and KI-450 (c), and K-500 and KI-500 (d).

thermal treatment compared to conventional calcination. This agreed with the reactivity results as well.

$^{1}$H MAS NMR was implemented to support evidence on the higher dehydroxylation rate phenomenon for KI complexes by comparing the hydroxylic groups release evolution of K and KI at 500 °C (Fig. 11). Kaol presents two typical peaks at around 2.5 ppm and 1.9 ppm, which are assigned to inner-surface hydroxyls and inner hydroxyls, respectively (Huittinen et al., 2013). Inner hydroxyls are established on the Al octahedra only, whereas inner-surface hydroxyls are bonded to the Al and Si sheets simultaneously to attach the different kaolinite sheets by hydrogen bonds. Therefore, inner hydroxyls exhibit higher electron density around the proton since they are not bonded to other chemical groups (Huittinen et al., 2013; Zhu et al., 2016). Moreover, at ~7 ppm, a broad resonance is observed, attributed to the adsorbed water within the kaolinitic structure (Mañosa et al., 2023). KI-500 shows a significant intensity decrease in both OH peaks compared to those in K-500. This supports the TGA results, indicating a major OH removal achieved for K-KAc complexes than raw kaolin when calcined.

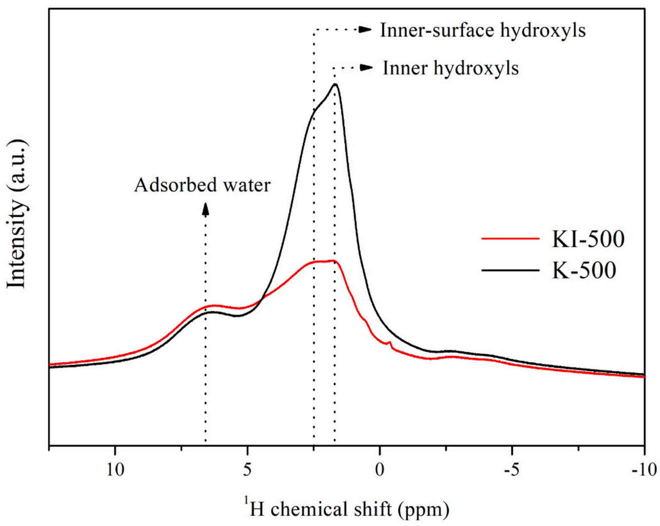

**Fig. 11.** $^{1}$H MAS NMR of K-500 and KI-500.

## 4. Conclusions

This study aimed to develop novel activation methods for kaolinite that reduce environmental impact. The main objective was to implement KAc intercalation within the kaolinite structure to enable the production of metakaolin at lower calcination temperatures. By achieving effective dehydroxylation at reduced temperatures, the study aimed to decrease energy consumption associated with the traditional production of metakaolin. The main outcomes of this study are summarized in the following key findings:

- The intercalation procedure achieved an 89% successful insertion, according to XRD results. Even though SEM revealed a conformational change in the intercalated kaolinite, its lamellar distribution was preserved. TGA showed the different dehydrxoylation onsets, with lower temperatures for intercalated complexes compared to kaolinite as a consequence of the OH exposal due to the lamellar expansion.
- The reactivity tests supported an increased pozzolanic activity for calcined KIs in comparison with calcining K. The modified Chapelle test and the Si/Al availability test results exposed that at 400, 450, and 500 °C, the KI complexes reactivity performances are higher than K.
- The intercalated kaolinite enhanced reactivity was elucidated through an exhaustive structural characterization. XRD analysis revealed a severe decrease in the kaolinitic reflections for the calcined KI series. Moreover, $^{27}$Al MAS NMR demonstrated changes in the Al surroundings at 450 and 500 °C, revealing a higher content of $Al^{V}$ and $Al^{IV}$ in KI compared to K. These findings explain the increase in amorphousness on the kaolinitic structure of the intercalated complexes.
- On the other hand, TGA served to quantify the dehydroxylation rate of the OH groups in KI and K samples. Calcining intercalated kaolinites in the range of 400 to 550 °C causes a significant increase in the dehydroxylation degree, achieving a higher content of amorphized material.

In conclusion, an enhancement of the kaolinitic reactivity is achieved by implementing a previous kaolinitic intercalation with KAc before calcining the material. This is caused by an easier OH removal produced because of the intercalation. In application terms, this could serve as a strategy to avoid high temperatures during metakaolin production, as it can be obtained preferentially at lower temperatures if intercalated.

## Funding

This work is partially supported by the Spanish Government with the

Grant PID2021-125810OB-C21 funded by MCIN/AEI/10.13039/501100011033 and by "ERDF A way of making Europe. The Catalan Government contributed with the Grant 2021 SGR 00708 through the Agència de Gestió d'Ajuts Universitaris i de Recerca (AGAUR).

## Approval of the submitted version of the manuscript

Please check this box to confirm that all co-authors have read and approved the version of the manuscript that is submitted. Signatures are not required.

## CRediT authorship contribution statement

**Adrian Alvarez-Coscojuela:** Writing – original draft, Visualization, Methodology, Investigation, Formal analysis, Data curation. **Josep Marco-Gibert:** Investigation, Formal analysis. **Jofre Mañosa:** Writing – review & editing, Supervision, Resources. **Joan Formosa:** Writing – review & editing, Funding acquisition. **Josep Maria Chimenos:** Writing – review & editing, Visualization, Supervision, Funding acquisition, Conceptualization.

## Declaration of competing interest

The authors declare that they have no known competing financial interests or personal relationships that could have appeared to influence the work reported in this paper.

## Data availability

Data will be made available on request.

## Acknowledgements

The authors would like to thank the Catalan Government for the quality accreditation given to their research group DIOPMA (2021 SGR 00708). DIOPMA is a certified agent TECNIO in the category of technology developers from the Government of Catalonia. The authors are grateful to the companies Minerals i Derivats, S.A. for the supply of the raw kaolin and the CCiTUB and SCAI for the equipment or measurements of SEM, ICP-OES, XRF, MAS NMR, and XRD. The authors acknowledge the support of CYTED Network ECoEICo—Circular Economy as a Strategy for a More Sustainable Construction Industry and the COST Action CircularB—Implementation of Circular Economy in the Built Environment.

## Appendix A. Supplementary data

Supplementary data to this article can be found online at https://doi.org/10.1016/j.clay.2024.107515.

## References

Alfonso, P., Penedo, L.A., García-Valles, M., Martínez, S., Martínez, A., Trujillo, J.E., 2022. Thermal behaviour of kaolinitic raw materials from San José (Oruro, Bolivia). J. Therm. Anal. Calorim. 147, 5413–5421. https://doi.org/10.1007/s10973-022-11245-3.

Alvarez-Coscojuela, A., Mañosa, J., Formosa, J., Chimenos, J.M., 2024. Structural characterisation and reactivity measurement of chemically activated kaolinite. J. Build. Eng. 87 https://doi.org/10.1016/j.jobe.2024.109051.

Benhelal, E., Zahedi, G., Shamsaei, E., Bahadori, A., 2013. Global strategies and potentials to curb $CO_2$ emissions in cement industry. J. Clean. Prod. 51, 142–161. https://doi.org/10.1016/j.jclepro.2012.10.049.

Bich, C., Ambroise, J., Péra, J., 2009. Influence of degree of dehydroxylation on the pozzolanic activity of metakaolin. Appl. Clay Sci. 44, 194–200. https://doi.org/10.1016/j.clay.2009.01.014.

Brigatti, M.F., Galán, E., Theng, B.K.G., 2013. Structure and Mineralogy of Clay Minerals. Development. Clay Sci. https://doi.org/10.1016/B978-0-08-098258-8.00002-X.

Cheng, H., Liu, Q., Yang, J., Du, X., Frost, R.L., 2010a. Influencing factors on kaolinite-potassium acetate intercalation complexes. Appl. Clay Sci. 50, 476–480. https://doi.org/10.1016/j.clay.2010.09.011.

Cheng, H., Liu, Q., Yang, J., Zhang, Q., Frost, R.L., 2010b. Thermal behavior and decomposition of kaolinite-potassium acetate intercalation composite. Thermochim. Acta 503–504, 16–20. https://doi.org/10.1016/j.tca.2010.02.014.

Cheng, H., Liu, Q., Cui, X., Zhang, Q., Zhang, Z., Frost, R.L., 2012a. Mechanism of dehydroxylation temperature decrease and high temperature phase transition of coal-bearing strata kaolinite intercalated by potassium acetate. J. Colloid Interface Sci. 376, 47–56. https://doi.org/10.1016/j.jcis.2012.02.065.

Cheng, H., Liu, Q., Yang, J., Ma, S., Frost, R.L., 2012b. The thermal behavior of kaolinite intercalation complexes-a review. Thermochim. Acta 545, 1–13. https://doi.org/10.1016/j.tca.2012.04.005.

Cheng, H., Li, K., Liu, Q., Zhang, S., Li, X., Frost, R.L., 2014. Insight into the thermal decomposition of kaolinite intercalated with potassium acetate: an evolved gas analysis. J. Therm. Anal. Calorim. 117, 1231–1239. https://doi.org/10.1007/s10973-014-3934-9.

Cheng, H., Zhang, S., Liu, Q., Li, X., Frost, R.L., 2015. The molecular structure of kaolinite-potassium acetate intercalation complexes: a combined experimental and molecular dynamic simulation study. Appl. Clay Sci. 116–117, 273–280. https://doi.org/10.1016/j.clay.2015.04.008.

Cheng, H., Liu, Q., Xu, P., Hao, R., 2018. A comparison of molecular structure and de-intercalation kinetics of kaolinite/quaternary ammonium salt and alkylamine intercalation compounds. J. Solid State Chem. 268, 36–44. https://doi.org/10.1016/j.jssc.2018.08.009.

Deng, Y., White, G.N., Dixon, J.B., 2002. Effect of structural stress on the intercalation rate of kaolinite. J. Colloid Interface Sci. 250, 379–393. https://doi.org/10.1006/jcis.2001.8208.

Fernandez, R., Martirena, F., Scrivener, K.L., 2011. The origin of the pozzolanic activity of calcined clay minerals: a comparison between kaolinite, illite and montmorillonite. Cem. Concr. Res. 41, 113–122. https://doi.org/10.1016/j.cemconres.2010.09.013.

Ferraz, E., Andrejkovičová, S., Hajjaji, W., Velosa, A.L., Silva, A.S., Rocha, F., 2015. Pozzolanic activity of metakaolins by the French standard of the modified Chapelle test: a direct methodology. Acta Geodyn. Geomater. 12, 289–298. https://doi.org/10.13168/AGG.2015.0026.

Frost, R.L., Locos, O.B., Kristof, J., Kloprogge, J.T., 2001. Infrared spectroscopic study of potassium and cesium acetate-intercalated kaolinites. Vib. Spectrosc. 26, 33–42. https://doi.org/10.1016/S0924-2031(01)00108-4.

Gabor, M., Toth, M., Kristf, J., Komaromi-hiller, G.I., 1995. Thermal behavior and decomposition of intercalated kaolinite, 43, 223–228.

Gartner, E., 2004. Industrially interesting approaches to "low-$CO_2$" cements. Cem. Concr. Res. 34, 1489–1498. https://doi.org/10.1016/j.cemconres.2004.01.021.

He, H., Ma, L., Zhu, J., Frost, R.L., Theng, B.K.G., Bergaya, F., 2014. Synthesis of organoclays: a critical review and some unresolved issues. Appl. Clay Sci. 100, 22–28. https://doi.org/10.1016/j.clay.2014.02.008.

Horte, C.H., Becker, C., Kranz, G., Schiller, E., Wiegmann, J., 1988. Thermal decompositions of kaolinite intercalation compounds. J. Therm. Anal. 33, 401–406. https://doi.org/10.1007/BF01913914.

Horváth, E., Kristóf, J., Frost, R.L., 2010. Vibrational spectroscopy of intercalated kaolinites. Part I. Appl. Spectrosc. Rev. 45, 130–147. https://doi.org/10.1080/05704920903435862.

Huittinen, N., Sarv, P., Lehto, J., 2013. A $^1$H and $^{27}$Al NMR investigation of yttrium(III) and europium(III) interaction with kaolinite. Appl. Clay Sci. 80–81, 182–188. https://doi.org/10.1016/j.clay.2013.04.005.

Johnston, C.J., Pepper, R.A., Martens, W.N., Couperthwaite, S., 2022. Relationship between thermal dehydroxylation and aluminium extraction from a low-grade kaolinite: Role of clay chemistry and crystallinity. Hydrometallurgy 214. https://doi.org/10.1016/j.hydromet.2022.105967.

Kuenzel, C., Ranjbar, N., 2019. Dissolution mechanism of fly ash to quantify the reactive aluminosilicates in geopolymerisation. Resour. Conserv. Recycl. 150, 104421 https://doi.org/10.1016/j.resconrec.2019.104421.

Lagaly, G., Ogawa, M., Dékány, I., 2013. Clay mineral-organic interactions. Development. Clay Sci. https://doi.org/10.1016/B978-0-08-098258-8.00015-8.

Li, Y., Sun, D., Pan, X., Zhang, B., 2009. Kaolinite intercalation precursors. Clay Clay Miner. 57, 779–786. https://doi.org/10.1346/CCMN.2009.0570610.

Li, X., Snellings, R., Antoni, M., Alderete, N.M., Ben Haha, M., Bishnoi, S., Cizer, Ö., Cyr, M., De Weerdt, K., Dhandapani, Y., Duchesne, J., Haufe, J., Hooton, D., Juenger, M., Kamali-Bernard, S., Kramar, S., Marroccoli, M., Joseph, A.M., Parashar, A., Patapy, C., Provis, J.L., Sabio, S., Santhanam, M., Steger, L., Sui, T., Telesca, A., Vollpracht, A., Vargas, F., Walkley, B., Winnefeld, F., Ye, G., Zajac, M., Zhang, S., Scrivener, K.L., 2018. Reactivity tests for supplementary cementitious materials: RILEM TC 267-TRM phase 1. Mater. Struct./Mater. Construct. 51 https://doi.org/10.1617/s11527-018-1269-x.

Mako, É., Kovács, A., Horváth, E., Kristóf, J., 2014. Kaolinite-potassium acetate and halloysite-potasium acetate complexes prepared by mechanochemical, solution and homogenization techniques: a comparative study. Clay Miner. 49, 457–471. https://doi.org/10.1180/claymin.2014.049.3.08.

Mañosa, J., Gómez-Carrera, A.M., Svobodova-Sedlackova, A., Maldonado-Alameda, A., Fernández-Jiménez, A., Chimenos, J.M., 2022. Potential reactivity assessment of mechanically activated kaolin as alternative cement precursor. Appl. Clay Sci. 228 https://doi.org/10.1016/j.clay.2022.106648.

Mañosa, J., la Rosa, J.C., Silvello, A., Maldonado-Alameda, A., Chimenos, J.M., 2023. Kaolinite structural modifications induced by mechanical activation. Appl. Clay Sci. 238, 106918 https://doi.org/10.1016/j.clay.2023.106918.

Ramezanianpour, A.A., Bahrami Jovein, H., 2012. Influence of metakaolin as supplementary cementing material on strength and durability of concretes. Constr. Build. Mater. 30, 470–479. https://doi.org/10.1016/j.conbuildmat.2011.12.050.

Ruiz Cruz, M.D., 1999. New Data on the Kaolinite-Potassium Acetate complex. Clay Miner. 34, 565–577. https://doi.org/10.1180/claymin.1999.034.4.05.

Sabir, B., Wild, S., Bai, J., 2001. Metakaolin and calcined clays as pozzolans for concrete: a review. Cem. Concr. Compos. 23, 441–454. https://doi.org/10.1016/S0958-9465(00)00092-5.

San Cristóbal, A.G., Castelló, R., Martín Luengo, M.A., Vizcayno, C., 2010. Zeolites prepared from calcined and mechanically modified kaolins. A comparative study. Appl. Clay Sci. 49, 239–246. https://doi.org/10.1016/j.clay.2010.05.012.

Schneider, M., Romer, M., Tschudin, M., Bolio, H., Worrell, E., Price, L., Martin, N., Hendriks, C., Meida, L.O., Gartner, E.M., Benhelal, E., Zahedi, G., Shamsaei, E., Bahadori, A., Scrivener, K.L., John, V.M., Gartner, E.M., Shan, Y., Guan, D., Zheng, H., Ou, J., Li, Y., Meng, J., Mi, Z., Liu, Z., Zhang, Q., 2018. Sustainable cement production-present and future. Cem. Concr. Res. 41, 142–161. https://doi.org/10.1016/j.jclepro.2012.10.049.

Scrivener, K.L., John, V.M., Gartner, E.M., 2018. Eco-efficient cements: potential economically viable solutions for a low-$CO_2$ cement-based materials industry. Cem. Concr. Res. 114, 2–26. https://doi.org/10.1016/j.cemconres.2018.03.015.

Shvarzman, A., Kovler, K., Grader, G.S., Shter, G.E., 2003. The effect of dehydroxylation/amorphization degree on pozzolanic activity of kaolinite. Cem. Concr. Res. 33, 405–416. https://doi.org/10.1016/S0008-8846(02)00975-4.

Siddique, R., Klaus, J., 2009. Influence of metakaolin on the properties of mortar and concrete: a review. Appl. Clay Sci. 43, 392–400. https://doi.org/10.1016/j.clay.2008.11.007.

Tironi, A., Trezza, M.A., Irassar, E.F., Scian, A.N., 2012. Thermal Treatment of Kaolin: effect on the Pozzolanic activity. Procedia Mater. Sci. 1, 343–350. https://doi.org/10.1016/j.mspro.2012.06.046.

Tironi, A., Trezza, M.A., Scian, A.N., Irassar, E.F., 2013. Assessment of pozzolanic activity of different calcined clays. Cem. Concr. Compos. 37, 319–327. https://doi.org/10.1016/j.cemconcomp.2013.01.002.

Walkley, B., Provis, J.L., 2019. Solid-state nuclear magnetic resonance spectroscopy of cements. Mater. Today Adv. 1, 100007 https://doi.org/10.1016/j.mtadv.2019.100007.

Xu, H., Wang, M., Liu, Q., Chen, D., Wang, H., Yang, K., Lu, H., Zhang, R., Guan, S., 2011. Stability of the compounds obtained by intercalating potassium acetate molecules into kaolinite from coal measures. J. Phys. Chem. Solids 72, 24–28. https://doi.org/10.1016/j.jpcs.2010.10.019.

Xu, H., Wang, M., Liu, Q., Chen, D., Wang, H., Yang, K., Lu, H., Zhang, R., Guan, S., Cheng, H., Zhang, S., Liu, Q., Li, X., Frost, R.L., Locos, O.B., Kristof, J., Kloprogge, J. T., 2015. The molecular structure of kaolinite-potassium acetate intercalation complexes: a combined experimental and molecular dynamic simulation study. Appl. Clay Sci. 116–117, 273–280. https://doi.org/10.1016/j.jpcs.2010.10.019.

Zeng, L., Cao, D., Yang Xu, Y., Fan, C. Wei, Peng, X. Qin, 2014. Novel method for preparation of calcined kaolin intercalation compound-based geopolymer. Appl. Clay Sci. 101, 637–642. https://doi.org/10.1016/j.clay.2014.09.034.

Zhong, X., Hua Liu, Y., Xu, T., Liu, W. Yuan, 2017. Studies on the thermal behavior and decomposition mechanism of dickite–potassium acetate complexes. J. Therm. Anal. Calorim. 129, 1095–1102. https://doi.org/10.1007/s10973-017-6266-8.

Zhu, X., Zhu, Z., Lei, X., Yan, C., 2016. Defects in structure as the sources of the surface charges of kaolinite. Appl. Clay Sci. 124–125, 127–136. https://doi.org/10.1016/j.clay.2016.01.033.